Laser and Particle Beams (2014), *32*, 89–97.
© Cambridge University Press, 2014 0263-0346/14 $20.00
doi:10.1017/S0263034613000906

Spatial extension of the electromagnetic field from tightly focused ultra-short laser pulses

L. IONEL[1] AND D. URSESCU[1,2]

[1]National Institute for Lasers, Plasma and Radiation Physics, Măgurele, jud. Ilfov, Romania
[2]"Horia Hulubei" National Institute for Physics and Nuclear Engineering, Măgurele, jud. Ilfov, Romania

(Received 12 August 2013; Accepted 31 October 2013)

Abstract

It is shown that in the focus of ultra-short pulses of duration *t*, the equivalent relation $s = ct$, where *c* is the speed of light and *s* the spatial extent of the pulse of the collimated pulse, does not hold. While the duration of one pulse is constant and independent of the measurement point, the spatial extension of the ultra-short pulse can be spatially shorter a factor more than 10 compared to the one obtained from the usual relation. The result is explained in correspondence with the extension of the Rayleigh range. Few femtosecond long gamma bursts can thus be generated in Thomson backscattering experiments performed in the lambda cube regime.

Keywords: Gaussian beam; Rayleigh range; Ultra-short pulses; Wavelength-cubed focal volume

1. INTRODUCTION

Understanding the behavior of matter in electric and magnetic fields remains a central point of interest in science. Extreme electric fields up to the 10^{16} V/cm exist in the vicinity of multiple ionized heavy nuclei, but in tiny volumes, less than cubic Angstrom (Winters & Stoehlker, 2009). Complementary, strong fields at the micrometer scale can be produced using lasers. Since 1960s, the laser produced fields strength registered an exponential increase, based on three directions of development, namely, the reduction of the pulse duration, of the focal spot area, and the increase of the pulse energy.

Following energy up-scaling path, several multi-PW facilities are proposed (e.g., Hays *et al.* (2007)), or under construction (extreme light infrastructure, Apollon laser in France, Vulcan-10 PW system in United Kingdom (Mourou *et al.*, 2011), exawatt center for extreme light studies in Russia (http://www.xcels.iapras.ru)) to investigate new physics effects down to the attosecond and possibly zeptosecond (10^{21} s) time scales and to promote new technologies based on ultra-short pulses of high energy photons, electrons, protons, neutrons, positrons, muons and neutrinos, on demand (Mourou *et al.*, 2006).

Address correspondence and reprint requests to: D. Ursescu, National Institute for Lasers, Plasma and Radiation Physics, Atomistilor 409, Magurele RO-077125, Măgurele, jud. Ilfov, Romania. E-mail: daniel.ursescu@eli-np.ro

Complementary, many experiments involve high focal intensities with less pulse energy, which also allows a high repetition rate operation (Hou *et al.*, 2006). In recent years, the relativistic intensity was produced in the kilohertz regime with short pulses of less than 10 fs composed of only a few electro-magnetic field cycles (Naumova *et al.*, 2004*a*). By focusing few cycles' laser pulses to diffraction limited spot, relativistic intensities can be achieved with milijoule energies (Naumova *et al.*, 2004*b*). While in this case both temporal and spatial extensions of the pulse are comparable with the wavelength of the pulse, the experiments using such pulses are also labeled as performed in the lambda cubed regime (λ^3) or wavelength cubed regime. Combining the spatial and temporal approaches, the planned extreme light infrastructure facility (Mourou *et al.*, 2011) will break into the ultra-relativistic regime and beyond, in generation of particles from the vacuum (polarization and boiling of the vacuum experiments). For such experiments, huge electric fields have to be created using tightly focused ultra-short laser pulses (TFP), i.e., in λ^3 regime. The effects expected in such experiments depend on the spatial and temporal extension of the huge electric fields generated by TFPs. Our paper provides here an analysis of the extension of the electromagnetic field in tightly focused ultrashort laser pulses used for experiments in the wavelength-cubed regime, relevant for experiments proposed at the ELI facility (Habs *et al.*, 2010).

In special relativity theory, the temporal τ and spatial σ coordinates are linked through the speed of light *c*.

$$\sigma = c \times \tau. \tag{1}$$

For laser pulses, their spatial extent along the propagation path and their duration are linked through a similar relation, in most cases. However, in this paper, it is shown that the relation mentioned above does not hold for linking spatial extent and temporal duration of tightly focused beams. Also, the evaluation of the spatial extension of the pulse in the focus is provided. It is also shown that a λ^3 regime can be achieved with significantly longer duration pulses. This effect is explained in connection with the associated Rayleigh range. As a consequence, it is shown that the Rayleigh length can limit drastically the presence of the high fields in TFP.

The obtained results find their use in the planning of experiments that combine ultra-short laser pulses and relativistic particle beams or other types of radiation. Such experiments include photon-photon interactions (Marklund & Shukla, 2006), probing the pair creation from the vacuum in the focus of strong electrical fields with γ- or electron beams, studies concerning the real part of the index of refraction of the vacuum in high fields (vacuum birefringence), production of cascades of e + e pairs and γ-rays triggered by a single slow electron in strong fields, Compton scattering and radiation reaction of a single electron at high intensities (Habs *et al.*, 2010), and entirely light based quantum double-slit experiments (King *et al.*, 2010). A direct result to be addressed here is related to the generation of few femtoseconds long gamma bursts in Thomson backscattering experiments based on TFPs and laser driven electron bunches. The sketch of such an experimental set-up at forthcoming ELI-NP facility (Habs *et al.*, 2010) is provided.

2. HOW TIGHT SHOULD ONE FOCUS?

The starting point of our analysis is the peak intensity to be reached in the focus of the TFP at existing or planned facilities. The highest intensity reported to date is 2×10^{22} W/cm^2 using a paraboloid with f-number $f\# = 1.0$ at the HERCULES 300 TW laser facility (Yanovsky *et al.*, 2008), but planned facilities aim to reach above 10^{23} W/cm^2. Such intensities will be achieved with laser pulses in the near infrared with pulse duration in the range of 10 fs to 200 fs and pulse energies in the range of 50–2000 J, corresponding to powers from 10 PW to 100 PW. From these parameters, one can roughly evaluate the focal f-number of the focusing optics needed in order to reach such intensities. Following (Siegman, 1986), the formula for the peak intensity in the focus of a Gaussian beam is:

$$I = 2P/\pi w_0^2, \tag{2}$$

where *I* is the peak intensity, *P* is the peak power and w_0 is the waist of the Gaussian beam. To connect this relation to the focusing element, we have to use the f-number relation:

$$w_0 = f\#\lambda, \tag{3}$$

where λ is the laser wavelength. Combining the relations of Eqs. (2) and (3), one can extract the dependence of the $f\#$ from the peak intensity of the laser pulses:

$$f\# = 1/\lambda(2P/\pi I)^{1/2}. \tag{4}$$

Figure 1 shows the f-number parameter for the focusing system needed to obtain a given beam intensity for ideal Gaussian pulses at the 800 nm wavelength, for 300 TW, 1 PW, 10 PW, and 100 PW peak power pulses. The highest intensity measured (Yanovsky *et al.*, 2008), obtained with a 300 TW laser system and a system with $f\# = 1$, is also represented with the star symbol. The horizontal (thick full) axis indicates focusing systems with $f\# = 0.5$, corresponding to cases where the beam radius equals the focal distance of the system. At lower $f\#$ values, the focus of the system is no more separated by the incoming beam path, even at 90° deflection. The essential conclusion that comes out from the Figure 1 is that reaching intensities above 10^{23} W/cm^2 needs not only high power systems but also focusing systems with the f-number as low as possible, corresponding to TFP. From the same plot one can estimate the beam waist w_0 with the help of Eq. (3), assuming a wavelength of 800 nm. The beam diameter remains of the order of the micrometer in the TFP configurations, making difficult the overlap of such pulses.

3. SPATIO-TEMPORAL EXTENSION IN TIGHTLY FOCUSED BEAMS

Analytical solutions for the electromagnetic field distribution of focused Gaussian laser beams are studied in the recent years in relation with charged particle acceleration mechanisms in vacuum. Solutions for monochromatic laser pulses are used most of the time, corresponding to infinite pulse

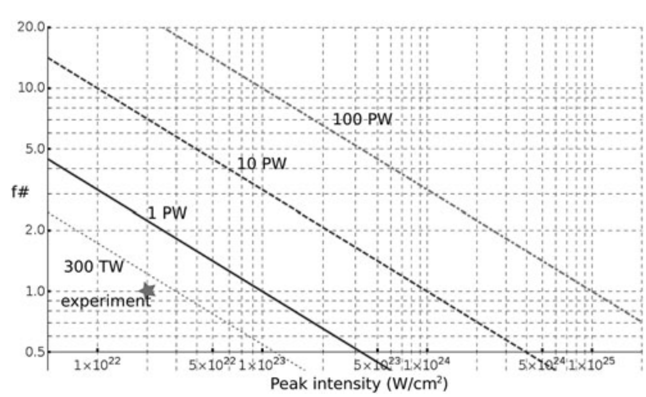

Fig. 1. f-number values for the focusing optics to obtain peak intensities in the ultra-relativistic regime.

durations. The solutions are infinite power series in the small parameter $\varepsilon = 1/(k\ w)$ used in the computations is usually limited to small values below $\varepsilon = 0.032$, corresponding to about 7° beam divergence and f-number of 5 (Quesnel & Mora, 1998). Even in this case, the use of fifth order terms is necessary for the accurate evaluation of the fields with waist dimensions down to 5 µm (Salamin & Keitel, 2002). For the ultra-short pulses, an analytical solution is presented in Quesnel and Mora (1998); the analytical solution is truncated and the validity of the solution is related to the condition that the laser pulse contains a large number of periods (at least 60 fs pulses).

As shown in the previous section, to reach the highest fields for experiments planned at multi-PW facilities such as ELI, one needs tighter focusing of the pulses, beyond the approximation in the analytical solutions from (Quesnel & Mora, 1998). So, in the evaluation below, we complement and extend the results concerning the electromagnetic field structure for ultrashort pulses below the spatial and temporal limits mentioned above, using a numerical approach.

Numerical computation of the ultra-short pulses propagation was performed in order to investigate the electromagnetic field distribution in the vicinity of the focus. We used FullWAVE, a package of the commercial software RSoft (http://www.rsoftdesign.com) which solves the Maxwell equations using the finite difference time domain (FDTD) method. The geometry of the problem is depicted in Figure 2. The study implies a laser source (central wavelength λ of 800 nm, variable diameter source in the interval of 30 µm and 150 µm, pulse duration varying between 5 and 120 fs, vertical polarization, symmetrical position to the x axis) which propagates initially along the z axis. The laser pulse is focused by a spherical mirror which has the focal distance of 75 µm and the diameter of 160 µm. The pulse duration will be denoted τ, while the period of the pulse is denoted T. Due to symmetry considerations, the point P where the electric field is most intense for the entire temporal range simulated is placed along the propagation axis z. The position of the point P was identified, monitoring the electromagnetic field along the propagation axis z in several points, with a quarter of a wavelength accuracy. This allowed finding out also the moment t_0 when the maximum electric field $EP\ (t_0)$ is produced in the specified point P. The envelope full width at half maximum of the electric field $E(t)$ was found to be the same in any point of the xz plane including P (except for the vicinity of the mirror where the pulse and its reflection interfere), within 6% precision. This indicates that the pulse duration is a good parameter for the pulse description.

The structure of the electric field $E(x,z)$ was computed in the vicinity of the focal point. In Figure 3 we illustrate the electric field distribution in the focal point P, using false color coded plots, where blue shows the negative values, green represents the zero field, while the red shows the positive parts of the field. All the plots preserve the same spatial ranges, centered on the P point. In the upper part of Figure 3, which illustrated the following cases: pulse duration of two cycles τ = 2.5 T at $f\# = 2.5$ in the upper left figure and at $f\# = 0.5$ in the upper right figure. In the last case, the field is slightly narrower but has a similar extension along the propagation axis. This does not hold any more in the lower part of the Figure 3, where pulse duration of 59 cycles τ = 59 T at $f\# = 2.5$ in the lower left figure and at $f\# = 0.5$ in the lower right figure, while the structure of the electric field along the propagation axis z for $f\# = 2.5$ is significantly longer than the one with the $f\# = 0.5$. However, the electric field $E(x,z)$ for $f\# = 0.5$ at τ = 2.5 T and τ = 59 T is looking almost identical. This indicates that the spatial electric field structure $E(x, z)$, for tightly focused pulses is not always sensitive to the duration of the pulse. In the central plot of the Figure 3, the electric field for the intermediate case τ = 11.8 T and $f\# = 0.83$ was represented for comparison.

Further, in Figure 4, it is illustrated for this particular case (τ = 11.8 T and $f\# = 0.83$), the difference between the temporal evolution of the envelope of the electric field $EP\ (t)$ and the spatial extent of the field along the propagation axis $E(x = 0; z)$. For the representation of the spatial extent

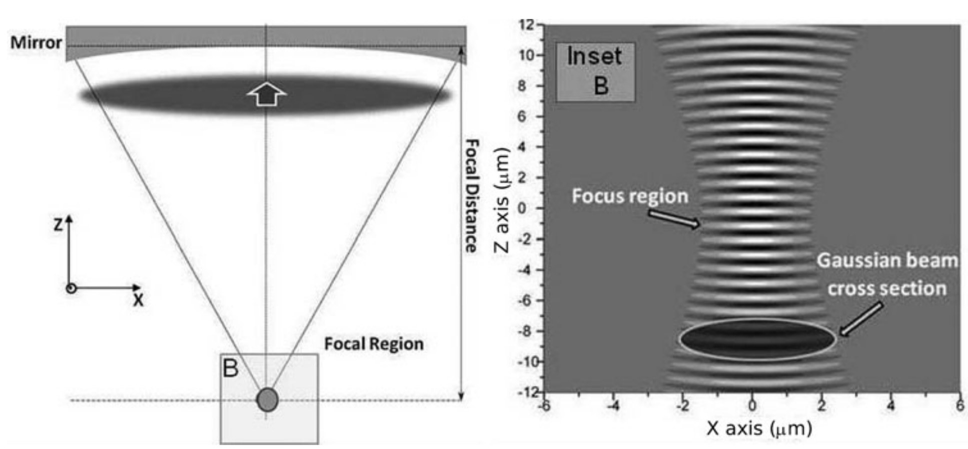

Fig. 2. Analyzed geometry and the fine structure of the field in the focal region. (**Left**) optical set up of the pulses focusing. (**Right**) Electromagnetic field distribution in focus in case of an extended source illustrating the Gaussian beam Ey distribution in the (xz) plane.

https://doi.org/10.1017/S0263034613000906 Published online by Cambridge University Press

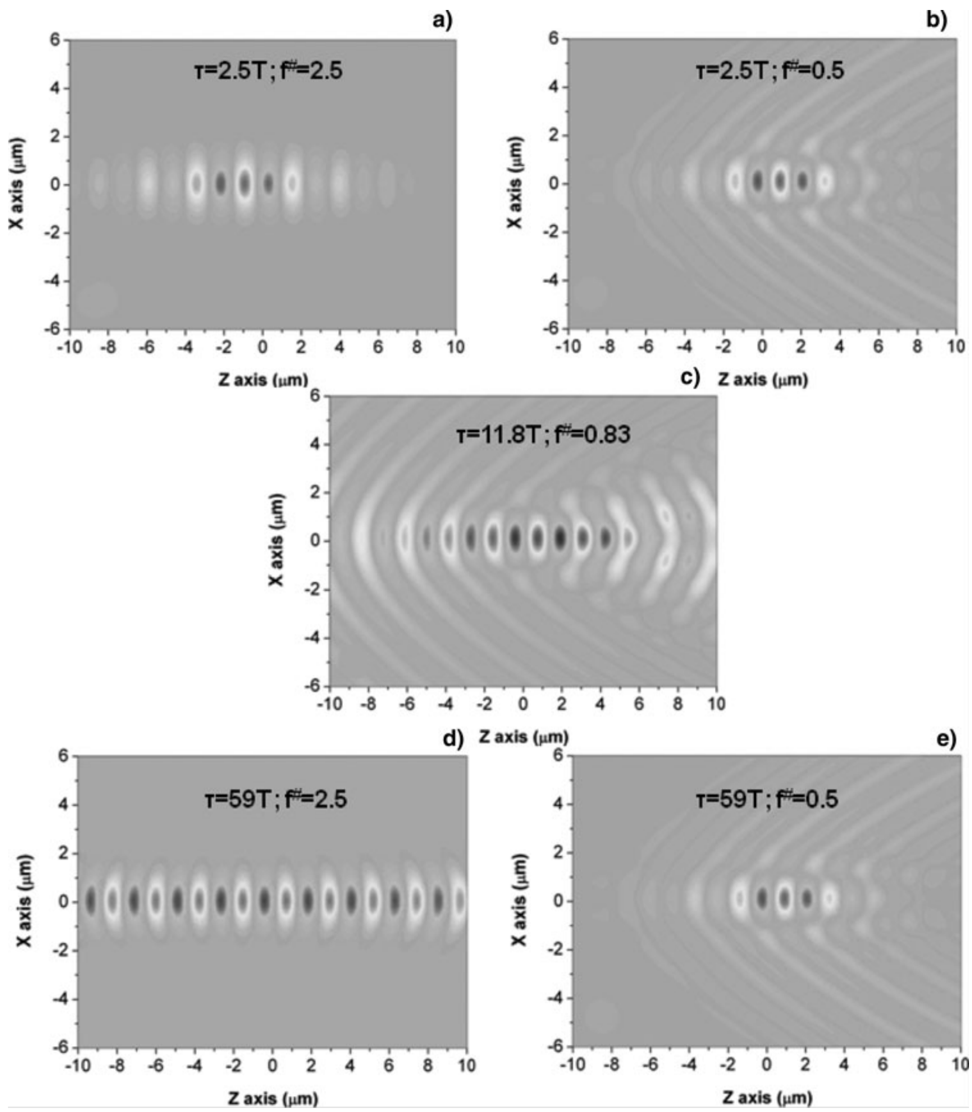

Fig. 3. The electromagnetic field distribution in the focal region for different pulse durations (τ) and for different diameters of the laser source (D): (**a**) τ = 2.5 T, laser D = 30 μm; (**b**) τ = 2.5 T, D = 150 μm; (**c**) τ = 11.8T, D =9 0 μm; (**d**) τ = 59 T, D = 30 μm; (**e**) τ = 59 T, D = 150 μm.

of the electric field along the z axis, the detailed field structure is represented at the time when the pulse reaches the focus.

For the temporal structure, we transformed the temporal axis into a spatial one using the Minkowski space relation from Eq. (1), and we represented the envelope of the temporal evolution for the electric field $E_P(t)$; in this case, 0 is the moment where the field reaches its maximum. The temporal envelope is a factor of 2.5 larger than the spatial one. One can also observe the signature of the spherical aberration in the soft modulation at the end of the spatial field structure.

In order to understand the effect, one can analyze the extension of the confocal region for TFP. The confocal parameter b equals two times the Rayleigh range of a Gaussian beam. Starting from the definition, the confocal parameter is described here as a function of the $f\#$, making use of Eq. (3):

$$b = 2\pi w_0^2/\lambda = 2\pi f\#^2\lambda \tag{5}$$

It can reach the same order of magnitude as the wavelength of the beam, as long as $f\#$ is of the order of unity. In this way, we obtain a confined spatial distribution of the electromagnetic field in a region of few cubic wavelengths, in the λ^3 regime. In order to characterize the discrepancy between the spatial and temporal extent of the TFP, we introduce a factor, denoted u that quantifies the relative spatial extension (RSE) of the TFP:

$$u = L_{FWHM}/(c\tau_{FWHM}), \tag{6}$$

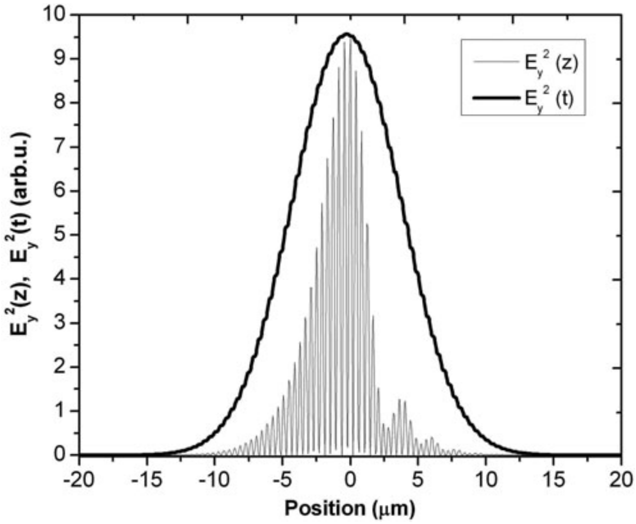

Fig. 4. Comparison of the temporal envelope with the spatial envelope for the square of the electric field from a TFP with an f-number of 0.83. The full width at half maximum of the spatial envelope is 3.78 μm while the temporal envelope has 9.35 μm/*c* duration, where *c* is the speed of light.

where L_{FWHM} and τ_{FWHM} are the full width at half maximum of the spatial extent of the pulses and temporal duration measured for Gaussian pulses in the focal plane.

We further performed a parametric study of the RSE as a function of τ_{FWHM} and *f*# of the assumed focusing system. The results are represented in Figure 5. For very short pulses, of few cycles, RSE is close to unity and is almost insensitive to *f*#. For longer pulses, the RSE decreases strongly, showing that spatial extension of the pulses can be up to a factor of 10 and smaller than the temporal one, in the case of 60 cycle's pulses and longer. Thus, even though the laser pulse might be longer, the high intensity region of the TFP remains similar in its spatial extension with the one provided with shorter pulses. Consequently, the pulses generated with high *f*# optics but somewhat longer pulses can be

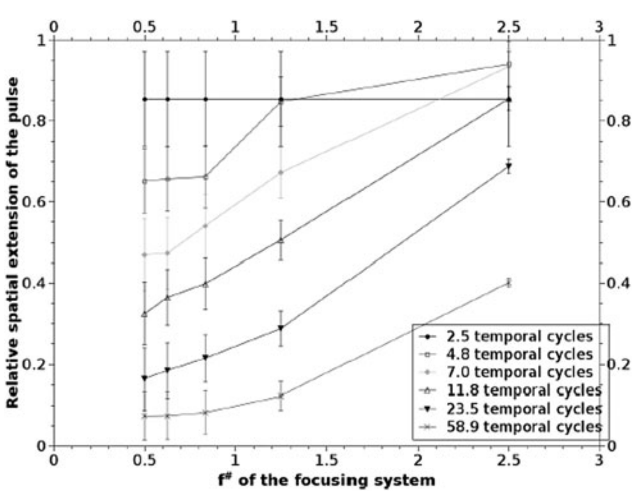

Fig. 5. Pulse length in focus, normalized with the number of cycles at the wavelength of 800nm as a function of the f-number.

understood as belonging to an extended lambda cubed regime.

4. ULTRA-INTENSE LASER FIELDS EXPERIMENTS IN THE EXTENDED LAMBDA CUBED REGIME

Eq. (6) for TFPs provided here can be used for the planning of the experiments performed in the lambda cube regime, namely, where the lasers can provide an energy encompassed in a focal volume of a few cubic wavelengths (λ^3). As shown in Section 2, this regime will be automatically achieved with existing or planned laser systems, once intensities of the order of 10^{23} W/cm^2 are targeted. Laser-gamma experiments and boiling of the vacuum experiments involving ultra-intense laser fields as proposed in Habs *et al.* (2010), Marklund and Shukla (2006), King *et al.* (2010) can be presently realized only using such TFPs.

Further in this section we limit ourselves to the analysis of experiments involving slow and fast electrons in TFPs, as a case study. This is motivated by the fact that experiments related to non-linear Thomson backscattering, Compton backscattering, laser driven electron acceleration in vacuum (Hora *et al.*, 2000; Gupta & Suk, 2007) and radiation reaction effects (Mao *et al.*, 2010) can be systematically performed at the ELI-NP facility to come online in 2017, and possibly other facilities. An exhaustive review of the processes can be found in (DiPiazza *et al.*, 2012)

The amplitude of the wiggling motion of an electron a_ω is given by:

$$a_\omega = eE/(m\omega^2) \tag{7}$$

where *e* is the absolute value of the electron charge, *E* represents the amplitude of the electric field, *m* is the electron mass, and ω is the angular frequency of the electromagnetic field (Brabec & Krausz, 2000; Pukhov, 2003) seen by the electron. The laser field amplitude formula is, following (Eliezer, 2002):

$$E = 2.75 \times 10^9 (I_L/10^{16} W/cm^2)^{1/2}. \tag{8}$$

Two cases can be identified, depending on the Doppler shift of the radiation as seen by the electron. In a first case, the wavelength seen by the electron is not Doppler shifted, as the electron is non-relativistic in the lab frame. In a second case, if the electron is relativistic, the Doppler shift can change the wavelength seen by the electron proportional with the relativistic Lorentz factor one or more orders of magnitude.

4.1. Non-Relativistic Electron in TFPs

Assuming linear polarized laser pulses within reach using existing technologies, the wiggling amplitude of the non-

https://doi.org/10.1017/S0263034613000906 Published online by Cambridge University Press

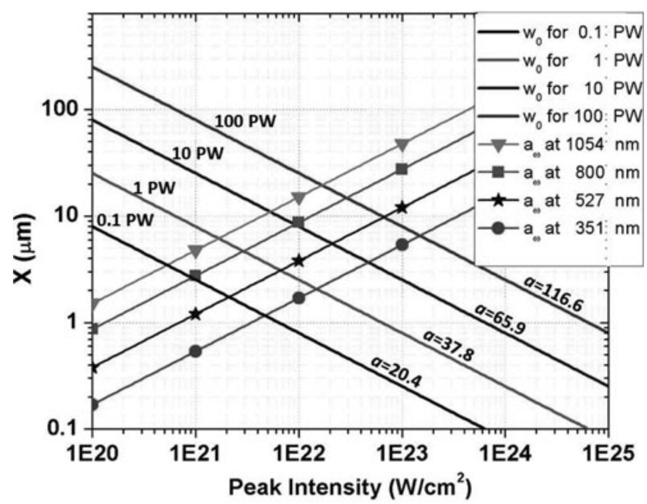

Fig. 6. The dependence of the Gaussian beam waist (w_0) and of the electron excursion amplitude (a_w) at a given intensity.

relativistic electron can reach values comparable or larger than the waist of the TFP, as illustrated in Figure 6. In such a case, the particles are violently accelerated and might easily escape in the transverse direction relative to the TFP direction of propagation. As a consequence, detecting such particles (as signature of the boiling of the vacuum, for example) has to be realized in the transverse plane. To find the onset of this process, Figure 6 illustrates the oscillation amplitude for a free and initially slow electron in TFP and the associated beam waist for the TFP.

When the amplitude of the oscillation becomes comparable with the waist, the infinite plane wave approximation is no longer valid. For example, at peak pulse power of 10 PW, at 800 nm wavelength, this takes place at intensities of 9×10^{21} W/cm^2, when the waist is about 9 μm. To achieve this intensity with ideal Gaussian beam, one needs to use optics with the *f*# of 10. If the pulse is short enough, below 20 cycles, the RSE factor is 1. For a 10 PW system at 351 nm, the corresponding waist is 10 μm, and the intensity reaches 5×10^{22} W/cm^2, achievable with *f*# of 4.6. In this case, the RSE factor is 0.8 for a 60 cycles pulse and smaller for longer pulses.

Conversely, for a system with *f*#1, the RSE factor is 0.4 in a 12 cycles pulse at 800 nm. The reached intensity is 10^{23} W/cm^2 and we are in a regime where the amplitude of the electron excursion during a single cycle in infinite plane wave approximation is about 30 μm while the waist is only 0.8 μm. Hence, the huge field in the focus will expunge the electrons from the intense field region in less than a half cycle in the transverse direction to the light propagation direction.

4.2. Relativistic Electron in TFPs

In the relativistic electron case counter-propagating a laser pulse, the Doppler shift changes the wavelength of the incoming radiation and, following Eq. (7), the amplitude of the oscillation is reduced proportional with the square of the Lorentz factor. In this case, the electron does not necessarily escape from the laser field in the transverse direction to laser propagation as in the case described in Section 4.1. As a consequence, harmonics generation experiments in the nonlinear Thomson scattering can be realized in ultra-intense laser fields, as reported to recent studies (Popa, 2008; 2009; 2011; 2012). The model described in Popa (2008) was used to perform computations using the plane wave approximation, so it can be used when the values of the *relativistic parameter a* ($a = eE/mc\omega$) are in the ultra-relativistic regime which correspond to beam intensities of the orders 10^{23} Wcm^{-2} and the waist is large enough in comparison with the wavelength of the laser field in the electron rest framework reference. According to the numerical model presented in (Popa, 2008; 2009; 2011) we evaluated the spectral intensity of the scattered radiation in case of 10 PW output power with the correspondent value of the relativistic parameter $a = 65.9$.

At the E7 experimental area of ELI-NP facility, two synchronous beams of 10 PW each and pulse duration below 25 fs are planned to be delivered at a repetition rate of one shot per minute. In addition, laser-synchronous electron bunches with energies up to 700 MeV and pulse durations in few picosecond ranges will be provided by a linear accelerator that drives a Thomson backscattering gamma beam source (GBS). The GBS follows the development of Thomson backscattering sources recently reported (Hartemann *et al.*, 2004; Chouffani *et al.*, 2006; Priebe *et al.*, 2008).

Following previous considerations, we analyzed the interaction between relativistic electrons (700 MeV) and a Ti-Sapphire laser beam ($\lambda = 800$ nm), in a configuration shown in Figure 7, planned to be available at E7 experimental area at ELI-NP. For this, we considered the equation of the energy of the quanta of the fundamental X radiation, described by:

$$W_j = j \times W_x = j(W_L \times \gamma_0^2 \times (1 + |\beta_0|)^2), \qquad (9)$$

where

$$\gamma_0 = We/mc^2, \qquad (10)$$

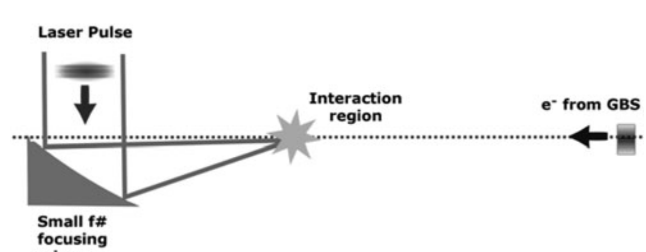

Fig. 7. Laser-GBS nonlinear Compton scattering set-up at E7 experimental area of ELI-NP.

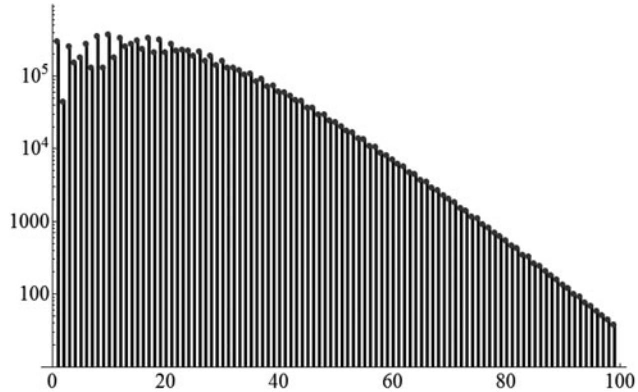

Fig. 8. The spectrum of the normalized total scattered radiation for $a = 65.9$ by computing the values of I_j as a function of j.

$$\beta_0 = (1 - 1/\gamma_0^2)^{1/2}, \quad (11)$$

and W_L *is* the laser energy, multiplied by the number of generated harmonics denoted by *j*. The study is performed close to 180° geometry, where the laser beam and the electron beam collide head-on with each other. As it can be seen in Figure 8, the maximum intensity is obtained by the 10th harmonic. Thus the energy of the quanta of the fundamental radiation can achieve up to 121, 5 MeV, with significant harmonics production also above 40th harmonic, in the 500 MeV range, neglecting the electron recoil. The generation of such quanta presents a great interest for many recent approaches in terms of high-intense laser fields, such as gamma ray assisted laser boiling of the vacuum (Habs *et al.*, 2010).

The use of the up to 700 MeV electron beam available at the ELI-NP facility has the drawback of low electron density in the bunch, as the planned electron bunch duration is of the order of 2 ps, and total charge in the range of 100 pC, similar to values reported in (Hartemann *et al.*, 2004). In order to increase the electron bunch charge density and to decrease the bunch length, laser driven electron bunches can be produced with energies from 100 MeV (Glinec *et al.*, 2005) up to 2 GeV (Wang *et al.*, 2013). The behavior of dense and short electron bunches compared to the wavelength of the intense laser field was modeled in (Smorenburg *et al.*, 2010). Such a set-up, also proposed earlier in (Kulagin *et al.*, 2008), using two synchronous 10 PW laser pulses, one to generate dense bunch of electrons in a gas jet and one for Compton is described in Figure 9.

Attosecond pulses generation through Thomson scattering was proposed earlier (Lee & Cha, 2003; Zhang *et al.*, 2008; Liu *et al.*, 2010). As the pulse duration of the produced gamma radiation is determined by the convolution of the electron bunch duration with the TFP spatial extension. If the electron bunch is significantly shorter than the duration of the TFP, then the Compton backscattered harmonics pulse duration will be determined by the electron bunch duration. This can be the case in experiments using laser accelerated electron bunches where the bunch length can reach durations of the order of 2 fs (Buck *et al.*, 2011; Lundh *et al.*, 2011). In such a case, covered by the set-up described in Figure 9, even using hundreds of femtosecond long pulse duration will provide Compton backscattered pulses with duration in the few femtosecond range.

5. CONCLUSIONS

As pointed out in the first part of this article, TFPs are needed in order to perform experiments in the ultra-relativistic regime with the existing or planned laser facilities. Spatial s and temporal t extensions of TFPs were investigated.

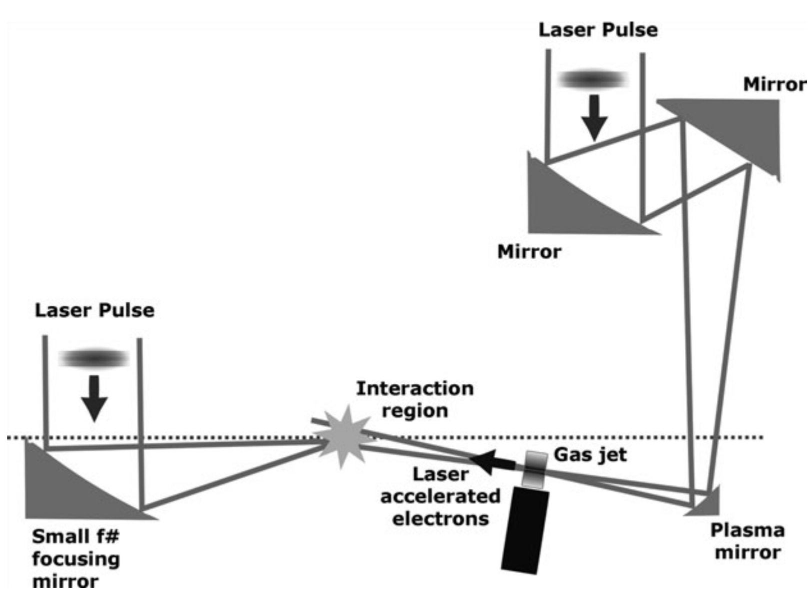

Fig. 9. Laser-only Compton backscattering set-up at E7 experimental area of ELI-NP.

Analytical solutions for the electric and magnetic fields are computational intensive, so FDTD numerical computation was used instead. The results show that the spatial extent of the EM field in focus of ultra-short pulses depends on Rayleigh range and it is shorter than the temporal duration of the pulse $c \times T$. A factor that quantifies the relative spatial extension (RSE) of the electromagnetic field of the laser pulse in the focal region was introduced and the extended lambda-cubed regime was thus described.

This impacts on the realization of experiments in strong laser fields. This study is important for future ultra-short pulse laser experiments at laser facilities such as Extreme Light Infrastructure. The results show that, in a restricted sense, the λ^3 regime can be reached with significantly longer pulses.

We have shown that depending on the type of the electron, non-relativistic or relativistic, the transverse extension of the TFP or the longitudinal extension of the TFP can play a major role. In the first case, the electrons are expunged from the focal region perpendicular to the direction of propagation, while in the second case, Compton scattering on relativistic electron bunches, gamma radiation can be produced with very short pulse duration even when employing relatively long laser pulses.

ACKNOWLEDGEMENT

The authors acknowledge discussions with Dietrich Habs, Dino Jaroszynski, Olimpia Budriga, Madalina Boca, Viorica Florescu, and Alexandru Popa. Work performed with the financial support of LAPLAS 3 program from ANCS, Romania and of the UEFISCDI project PN2-Parteneriate-1/2012. This work is supported by Extreme Light Infrastructure – Nuclear Physics (ELI-NP) — Phase I, a project co-financed by the Romanian Gouvernment and European Union through the European Regional Development Fund.

REFERENCES

Brabec, T. & Krausz, F. (2000). Intense few-cycle laser fields: Frontiers of nonlinear optics. *Rev. Mod. Phys.* **2**, **72**, 545–591.

Buck, A., Nicolai, M., Schmid, K., Sears, C.M.S., Sävert, A., Mikhailova, J.M., Krausz, F., Kaluza, M.C. & Veisz, L. (2011). Real-time observation of laser-driven electron acceleration. *Nat. Phys.* **7**, 543–548.

Chouffani, K., Harmon, F., Wells, D., Jones, J. & Lancaster, G. (2006). Laser-compton scattering as a tool for electron beam diagnostics. *Laser Part. Beams* **24**, 411–419.

Eliezer, S. (2002). *The Interaction of High-Power Lasers with Plasmas* (John Navas, ed.). Bristol: IOP Publishing Ltd.

Glinec, Y., Faure, J., Pukhov, A., Kiselev, S., Gordienko, S., Mercier, B. & Malka, V. (2005). Generation of quasimonoenergetic electron beams using ultrashort and ultraintense laser pulses. *Laser Part. Beams* **23**, 161–166.

Gupta, D.N. & Suk, H. (2007). Electron acceleration to high energy by using two chirped lasers. *Laser Part. Beams* **25**, 31–36.

Habs, D., Gross, M., Marginean, N., Negoita, F., Thirolf, P.G. & Zepf, M. (2010). The white book of ELI-nuclear physics, the scientific case of ELI nuclear physic pillar. http://www.eli-np.ro/documents/ELI-NP-WhiteBook.pdf.

Hartemann, F., Tremaine, A., Anderson, S., Barty, C., Betts, S., Booth, R., Brown, W., Crane, J., Cross, R., Gibson, D., Fittinghoff, D., Kuba, J., Le Sage, G., Slaughter, D., Wootton, A., Hartouni, E., Springer, P., Rosenzweig, J. & Kerman, A. (2004). Characterization of a bright, tunable, ultrafast Compton scattering X-ray source. *Laser and Part. Beams* **22**, 221–244.

Hays, G.R., Gaul, E.W., Martinez, M.D. & Ditmire, T. (2007). Broad-spectrum neodymium-doped laser glasses for high-energy chirped-pulse amplification. *Appl. Opti.* **46**, 4813–4819.

Hora, H., Hoelss, M., Scheid, W., Wang, J.W., Ho, Y.K., Osman, F. & Castillo, R. (2000). Principle of high accuracy for the nonlinear theory of the acceleration of electrons in a vacuum by lasers at relativistic intensities. *Laser Part. Beams* **18**, 135–144.

Hou, B., Nees, J., Mordovanakis, A., Wilcox, M., Mourou, G., Chen, L., Kieffer, J.C., Chamberlain, C.C. & Krol, A. (2006). Hard X-ray generation from solids driven by relativistic intensity in the lambda-cubed regime. *Appl. Phys. B* **83**, 81–85.

King, B., Piazza, A.D. & Keitel, C.H. (2010). A matter less double slit. *Nat. Photon* **4**, 92–94

Kulagin, V.V., Cherepenin, V.A., Hur, M.S., Lee, J. & Suk, H. (2008). Evolution of a high-density electron beam in the field of a super-intense laser pulse. *Laser Part. Beams* **26**, 397–409.

Lee, K. & Cha, Y.H. (2003). Relativistic nonlinear Thomson scattering as attosecond X-ray source. *Phys. Rev. E* **67**, 026502.

Liu, L., Xia, C.-Q., Liu, J.-S., Wang, W.-T., Cai, Y., Wang, C., Li, R.-X. & Xu, Z.-Z. (2010). Generation of attosecond X-ray pulses via Thomson scattering of counter-propagating laser pulses. *Laser Part. Beams* **28**, 27–34.

Lundh, O., Lim, J., Rechatin, C., Ammoura, L., Ben-Ismaïl, A., Davoine, X., Gallot, G., Goddet, J.-P., Lefebvre, E., Malka, V. & Faure, J. (2011). Few femtosecond, few kiloampere electron bunch produced by a laser-plasma accelerator. *Nat. Phys.* **7**, 219–222.

Mao, Q., Kong, Q., Ho, Y., Che, H., Ban, H., Gu, Y. & Kawata, S. (2010). Radiative reaction effect on electron dynamics in an ultra intense laser field. *Laser Part. Beams* **28**, 83–90.

Marklund, M. & Shukla, P.K. (2006). Nonlinear collective effects in photon-photon and photon-plasma interactions. *Rev. Mod. Phys.* **78**, 591.

Mourou, G.A., Korn, G., Sandner, W. & Collier, J.L. (2011). *ELI – Extreme Light Infrastructure - Science and Technology with Ultra-Intense Lasers*. Berlin: THOSS Media GmbH.

Mourou, G.A., Tajima, T. & Bulanov, S.V. (2006). Optics in the relativistic regime. *Rev. Mod. Phys.* **78**, 309.

Naumova, N.M., Nees, J.A., Hou, B., Mourou, G.A. & Sokolov, I.V. (2004). Isolated attosecond pulses generated by relativistic effects in a wavelength-cubed focal volume. *Opt. Lett.* **29**, 778–780.

Naumova, N.M., Nees, J.A., Sokolov, I.V., Hou, B. & Mourou, G.A. (2004). Relativistic generation of isolated attosecond pulses in a lambda^3 focal volume. *Phys. Rev. Lett.* **92**, 063902

Piazza, D.A., Müller, C., Hatsagortsyan, K.Z. & Keitel, C.H. (2012). Extremely high-intensity laser interactions with fundamental quantum systems. *Rev. Mod. Phys.* **84**, 1177–1228.

Popa, A. (2008). Accurate calculation of high harmonics generated by relativistic Thomson scattering. *J. Phys. B: At. Mol. Opt. Phys.* **41**, 015601/1–7.

Popa, A. (2009). Modeling properties of hard X-rays generated by the interaction between relativistic electrons and very intense laser beams. *J. Phys. B: At. Mol. Opt. Phys.* **42**, 025601/1–9.

Popa, A. (2011). Periodicity property of relativistic Thomson scattering with application to exact calculations of angular and spectral distributions of the scattered field. *Phys.l Rev. A* **84**, 023824.

Popa, A. (2012). Polarization effects in collisions between very intense laser beams and relativistic electrons. *Laser Part. Beams* **30**, 591–603.

Priebe, G., Laundy, D., Macdonald, M.A., Diakun, G.P., Jamison, S.P., Jones, L.B., Holder, D.J., Smith, S.L., Phillips, P.J., Fell, B.D., Sheehy, B., Naumova, N., Sokolov, I.V., Ter-Avetisyan, S., Spohr, K., Krafft, G.A., Rosenzweig, J.B., Schramm, U., Gruner, F., Hirst, G.J., Collier, J., Chattopadhyay, S. & Seddon, E.A. (2008). Inverse Compton backscattering source driven by the multi-10 TW laser installed at Daresbury. *Laser Part. Beams* **26**, 649–660.

Pukhov, A. (2003). Strong field interaction of laser radiation. *Rep. Prog. Phys.* **66**, 47–101.

Quesnel, B. & Mora, P. (1998). Theory and simulation of the interaction of ultraintense laser pulses with electrons in vacuum. *Phys. Rev. E* **58**, 3719.

Salamin, Y.I. & Keitel, C.H. (2002). Electron acceleration by a tightly focused laser beam. *Phys. Rev. Lett.* **88**, 095005.

Siegman, A.E. (1986). *Lasers* (Aidan, Kelly, ed.). South Orange: University Science Books.

Smorenburg, P., Kamp, L., Geloni, G. & Luiten, O. (2010). Coherently enhanced radiation reaction effects in laser-vacuum acceleration of electron bunches. *Laser Part. Beams* **28**, 553–562.

Wang, X., Zgadzaj, R., Fazel, N., Li, Z., Yi, S.A., Zhang, X., Henderson, W., Chang, Y.-Y., Korzekwa, R., Tsai, H.-E., Pai, C.-H., Quevedo, H., Dyer, G., Gaul, E., Martinez, M., Bernstein, A.C., Borger, T., Spinks, M., Donovan, M., Khudik, V., Shvets, G., Ditmire, T. & Downer, M.C. (2013). Quasi-monoenergetic laser-plasma acceleration of electrons to 2 GeV. *Nat Commun.* **4**, 1988.

Winters, D.F.A. & Stoehlker, T. (2009). Atomic physics at storage rings: Recent results from the ESR and future perspectives at fair. *Internation. J. Mod. Phys. E* **18**, 359.

Yanovsky, V., Chvykov, V., Kalinchenko, G., Rousseau, P., Planchon, T., Matsuoka, T., Maksimchuk, A., Nees, J., Cheriaux, G., Mourou, G. & Krushelnick, K. (2008). Ultra-high intensity-300-TW laser at 0.1 Hz repetition rate. *Opt. Express* **16**, 2109–2114.

Zhang, P., Song, Y. & Zhang, Z. (2008). Attosecond pulse generation in Thomson scattering with phase-controlled few-cycle laser pulses. *Phys. Rev. A* **78**, 013811.